Earth Systems and Environment (2022) 6:681–696
https://doi.org/10.1007/s41748-021-00260-3

ORIGINAL ARTICLE

Hydro-climatic and Water Availability Changes and its Relationship with NDVI in Northern Sub-Saharan Africa

Faustin Katchele Ogou[1,2] · Vincent Nduka Ojeh[3] · Edward Naabil[4] · Chukwuemeka I. Mbah[5]

Received: 29 May 2021 / Revised: 24 September 2021 / Accepted: 25 September 2021 / Published online: 19 October 2021

Abstract

The variations in total water storage anomaly and groundwater balance were examined during 2002–2016. Based on the empirical orthogonal function, it was found that the water resource underwent high variability. The linear trend of hydro-climatic variables, total water storage anomaly, water budget, and its components have been investigated. For the area average, all the variables increased except for the potential evapotranspiration, which had decreased during the period of study. For the spatial distribution of trends in total water storage (TWS) in the northern Sub-Saharan Africa (NSSA), 44.76% underwent significant negative changes, whereas the proportion of areas that underwent significant negative changes was 24.84%. The results indicated that the precipitation and soil moisture were determinant factors for positive changes in TWS, whereas the potential evapotranspiration and temperature contributed to the reduction in TWS, respectively, implying a harmful effect of rising in temperature on water resources over the region. Moreover, a non-significant positive interdependence between the area-averaged TWS and the water budget (WB) was acquired. Positive correlations between normalized difference vegetation index (NDVI) and TWS (WB) occupied 48.93% (37.86%), but negative correlations occupied 34.59% (28.49%) of the total area. Results of the relationships between TWS and NDVI were higher than that of NDVI and water budget over the period 2002–2015. The TWS and WB (water resources) played essential roles in the positive changes in the ecosystem. These findings are valuable for the management of agriculture, water resources, environment**,** and ecosystem, profiting from the implementation of policies at regional and local scales.

Keywords Hydro-climatic variables · Total water storage · GLDAS · NDVI · Northern Sub-Saharan Africa

1 Introduction

Water resource and environment management remain a crucial challenge over the world mainly in the era of changing climate. The challenge of water and environments is particularly important in Africa where many activities are dependent on nature's willingness. While some regions are facing these challenges in crucial ways, others with good capacity-building developed adequate strategies. Northern Sub-Saharan Africa is one of the regions that suffered from water resource and environmental management. Therefore, the present work focuses on northern sub-Saharan Africa to provide insights into water resource changes and their relationship with vegetation cover. Climate change has been anticipated to affect the low- and middle-revenue countries most particularly a few decades to come, through increased flooding and droughts events (Tom et al. 2012). Land water reserve has been observed to contribute significantly to the regional water cycle of the West African region (Grippa

✉ Vincent Nduka Ojeh
vinceojehnetwork@gmail.com

1 Laboratory of Atmospheric Physics, Department of Physics, Faculty of Sciences and Technology, University of Abomey-Calavi, 01 BP: 526, Godomey, Republic of Benin

2 University of Chinese Academy of Sciences, Beijing 100049, China

3 Climate Science Unit, Department of Geography, Faculty of Social Sciences, Taraba State University, Jalingo PMB 1167, Nigeria

4 Department of Agricultural Engineering, Bolgatanga Polytechnic, Box 767, Bolgatanga, Ghana

5 Chief Research Fellow, External Conflict Prevention and Resolution Directorate, Institute for Peace and Conflict Resolution—Ministry of Foreign Affairs, Abuja, Plot 486, Abogo Largema Boulevard, Central Business District, Abuja, Nigeria

et al. 2011). It has been shown that the wet and dry events had increased over northern Sub-Saharan Africa (NSSA; Ogou et al. 2017). Precipitation has been discovered to be one of the critical factors in the water balance in a catchment; and hence, the water cycle is understood to be most sensitive to precipitation in regard to seasonal and annual variations (Petheram et al. 2002).

Apart from limited studies on total water storage (TWS) changes related to climate change, limited attention had been paid to the qualitative and quantitative investigations of hydro-climatic and NDVI effects on water resources particularly TWS and water budget over the NSSA. The precipitation patterns had been reported to be linked with the El Niño Southern Oscillation (ENSO) (Gizaw and Gan 2017). It was the leading driver of changes in interannual groundwater storage. Meanwhile, the Atlantic Multidecadal Oscillation (AMO) played a significant role in decadal to multidecadal variability (Carvalho et al. 2018) in water resource variations. The combined effects of ENSO and AMO could generate noteworthy fluctuations in recharge to the aquifers and groundwater storage specifically in the Sahel (Carvalho et al. 2018).

Although the impact of climate change has been found to be large over the region by many investigations, the determination of the magnitude of increase or decrease in precipitation remains a challenge for effective mitigation or resilience. Meanwhile, the direct and indirect impacts of demographic variation on both water resources and water demand were found to be insignificant with high confidence limits (Carter and Parker 2009). Therefore, the climate change effect is the most prominent in the study. The area of the study is shown in Fig. 1.

The detection of all the relevant hydrological variables that were indispensable for studying hydrological drought at temporal and spatial scales as well is challenging (Thomas et al. 2014). Previous researchers had used the total water storage (TWS) to typify regional floods and the capacity of the Gravity Recovery and Climate Experiment (GRACE) mission for additional hand-outs to regional water management, drought evaluation (Famiglietti and Rodell 2013; Reager and Famiglietti 2009). Estimated total water storage change in Cameroon during the period 1962–1993 has shown declining trends which had been explained in terms of decrease in precipitation (Guenang et al. 2016). In regard to the preceding descriptions, the main objectives of the paper are:

1. To test the capability of TWS in detecting floods and drought over the NSSA
2. To analyze the change in hydro-climatic and its association with water resources
3. To examine changes in water storage and water balance components in recent past decades
4. Compare the water budget from the GLDAS model to the observed satellite TWS and
5. Examine the relationship of TWS and water budget with vegetation cover changes (NDVI). The findings of the paper will be vital to enlighten the water management stakeholders for planning agricultural activities and implementation of relevant policies.

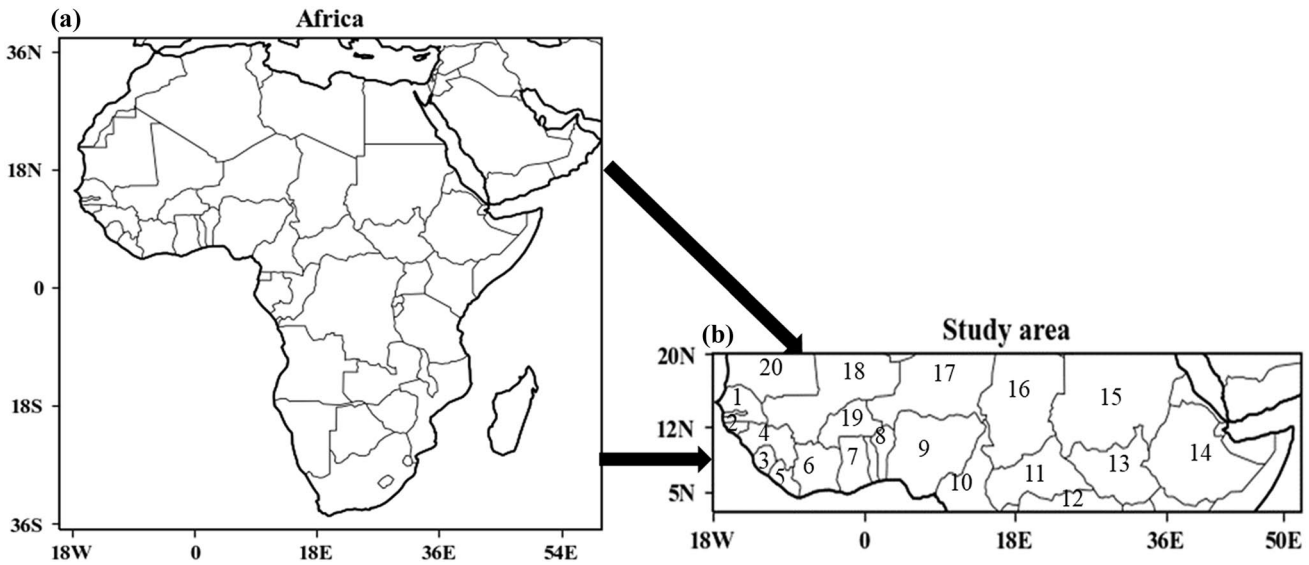

Fig. 1 The map of Africa showing: **(a)** The study area (**b**) The numbers representing the most visible countries. 1 = Senegal, 2 = Guinea-Bissau, 3 = Sierra Leone, 4 = Guinea (Conakry), 5 = Liberia, 6 = Ivory Coast, 7 = Ghana, 8 = Benin, 9 = Nigeria, 10 = Cameroun, 11 = Central African Republic, 12 = northern Congo, 13 = South Sudan, 14 = Ethiopia, 15 = Sudan, 16 = Chad, 17 = Niger, 18 = Mali, 19 = Burkina-Faso, 20 = Southern Mauritania

2 Data and Methods

2.1 Data

The Climate Prediction Center (CPC) soil moisture data of a single column of depth 16 cm provided by NCEP Reanalysis data provided by the NOAA/OAR/ESRL PSD, Boulder, Colorado, USA, from their Web site at https://www.esrl.noaa.gov/psd/ (Dool 2003) were used. The temporal coverage of the data was from 1948 to the near present at the spatial resolution of 0.5° × 0.5°. Likewise, the monthly soil moisture data were obtained from the Global Land Data Assimilation System (GLDAS) version 2.0, which employed the Noah land surface model (Cosgrove et al. 2004) with the spatial resolution of 0.25° × 0.25° and with the temporal coverage from 1981 to 2016 for comparison purpose. The horizontal resolution of total evapotranspiration (ET) and runoff (Ro) from GLDAS was 1°, and the temporal coverage is from 1979 to the near present. This ET presented a remarkable similarity with in-situ ET in the Lowess Plateau of China (Yang et al. 2016), which made the data reliable.

The high-resolution data of the world's meteorological stations over land areas are obtained from the Climatic Research Unit (CRU) of the University of East Anglia (Harris et al. 2014). The monthly precipitation (PRE), temperature (TMP), and potential evapotranspiration (PET) with a spatial resolution of 0.5° × 0.5° (longitude/latitude) are used. The temporal coverage of the datasets is from 1901 to 2016 and they are freely available at the following link: https://crudata.uea.ac.uk/cru/data/hrg/cru_ts_4.01/cruts.1709081022.v4.01/. Besides, the precipitation rate (RF) obtained from the Global Land Data Simulation (GLDAS) is used.

Three sources of monthly GRACE-derived, mainly the Gravity Recovery and Climate Experiment products version LND.RL05, which used the Goddard Earth Sciences Data and Information Services Center were downloaded from their website at http://grace.jpl.nasa.gov. These data were spherical harmonic solutions from the center for Space Research (CSR), geoForschingsZentrum (GFZ), and the Jet Propulsion Laboratory (JPL) covering April 2002 to December 2016. They were provided at a resolution of 1° × 1° along with associated leakage and measurement errors (Landerer and Swenson 2012) and pre-processed using the Gaussian method with a width of 300 km and a maximum degree of 60. The data sets were relevant for fields application, such as floods, drought, and groundwater monitoring (Looking to the Future: Forming a Comprehensive GRACE-FO Applications Strategy: Bolten et al. 2012).

Likewise, we collected the normalized difference vegetation index (NDVI) data sets from https://ecocast.arc.nasa.gov/data/pub/gimms/3g.v1/, which has a horizontal resolution of 1/12° × 1/12° and a temporal spanning from 1981 to 2015 (Pinzon and Tucker 2014). The dataset was generated from the Advanced Very High-Resolution Radiometers (AVHRR) Global Inventory Modelling and Mapping Studies (GIMMS) third-generation (NDVI3g) using an Artificial Neural Network-derived model. Before calculating the correlation, we have up-scaled the original resolution of NDVI to 1° × 1° to match with the resolution of TWS. The arithmetic means up-scaling method was applied (Zhang et al. 2017). The NDVI less or equal to zero was masked out before the analysis. The NDVI is used as a proxy for vegetation cover.

2.2 Methods

The multiple linear regression is used to reveal the relationship between water resources variables and hydro-climatic variables and NDVI.

The equation of average is defined as follows:

$$\overline{X}_i = \frac{\sum_{i=1}^{n} X_{ij}}{n} \tag{1}$$

where n is the total number of data and n is the number of samples data. In this analysis, using a least-square based on the linear regression technique, the spatial and temporal variations of the seasonal and annual climate variables and average seasonal and annual NDVI were studied. Empirical orthogonal function (EOF) analysis was applied to reveal the leading modes of the climate variables and to analyze the dynamic structures, trends, and oscillations of data (Hannachi 2004). The EOF as correlation consisted of the extraction of the principal component time series and correlated with the original anomalous data (Deser and Blackmon 1995). The EOF equation is expressed as follows:

$$f(x,t) = \sum_{i=0}^{m} f\left(x_i\right) \times PC_i(t) \tag{2}$$

where t is time, x is space, and i is the number of modes.

The term correlation used in statistics describes a linear statistical relationship between two random variables. The phrase "linear statistical indicated" that the mean of one of the random variables was dependent linearly upon the random variables of the other. The stronger is the relationship, the stronger is the correlation. The Pearson's correlation has been used by many authors (Du et al. 2015; Jonah et al. 2021). The given formula is as follows:

$$r = \frac{\sum_{i=1}^{n}\left(X_i - \overline{X}\right)\left(Y_i - \overline{Y}\right)}{\sqrt{\sum_{i=1}^{n}\left(X_i - \overline{X}\right)^2 \times \sum_{i=1}^{n}\left(Y_i - \overline{Y}\right)^2}} \tag{3}$$

where X_i is the annual value of each variable, $\overline{X}(\overline{Y})$ is the mean value of a variable in all years, Y_i is the annual of a climate factor (e.g., TMP, PRE, SM) in all years, n is the number of samples; r is the correlation coefficient between X_i and Y_i. The r is useful because it provides the degree of agreement between two variables.

The time series of each grid point was calculated to attain the slope coefficient based on the trend line. Precisely, the slope coefficients of the linear regression were worked out by employing the following equation (Jiang et al. 2017):

$$slope = \frac{n \times \sum_{n=1}^{n} X_i Y_i - \sum_{n=1}^{n} X_i \sum_{n=1}^{n} Y_i}{n \sum_{n=1}^{n} X_i^2 - \left(\sum_{n=1}^{n} X_i\right)^2} \quad (4)$$

where X_i and Y_i were the values of the independent variable and the dependent variable in the ith year, respectively, and n is the average number of years during the study period. Generally speaking, if slope > 0, the fluctuation of the dependent variable reveals an increase tendency, whereas if slope < 0, the fluctuation of the dependent variable reveals a decreasing tendency. The following equation represents the regression model used:

$$Y_i = aX_i + b + \varepsilon \quad (5)$$

where a represents the slope, b is the constant and ε is the residual error.

2.3 Water Budget Analysis

The water budget (WB) is estimated using the products from GLDAS, such as runoff (Ro), total evapotranspiration (ET) and the precipitation (RF) data, which have a horizontal resolution of 1° × 1°. It was noted that the precipitation from CRU is represented by PRE, while the precipitation from GLDAS is represented by RF. The RF was used because it has the same resolution and unit with ET and Ro. The estimation was based on the given water balance Eq. (7). The simplified equation of water balance (PRE–ET) (6), which has been considered as water yield (WY) (Feng et al. 2012; Lv et al. 2019) was also explored. It was noticed that each of these variables was multiplied by 86,400 s to convert initial units into units per day.

$$WY = RF - ET \quad (6)$$

$$WB = RF - ET - Ro \quad (7)$$

The source of TWS used afterwards in the study is chosen based on correlations between the three sources (GFZ, JPL and CSR). From the Fig. 2, we retained that of CSR.

3 Results and Discussion

3.1 Temporal Changes in the Total Water Storage and Climate Variables

Figure 3 depicted the linear trend in the time series of TWS, PRE, PET, TMP, and SM during 2002 − 2016. An increasing trend was observed in the TWS during the period of study (Fig. 3a). The increasing rate of 0.76 mm year^{-1} was obtained with a probability $p = 0.20$, implying that it is not significant at the 5% level. The increased tendency was explained by 61.19% of anomalous positive change in TWS. The increase rate observed in our study was comparable with that of the study of Guillaume et al. (2011),

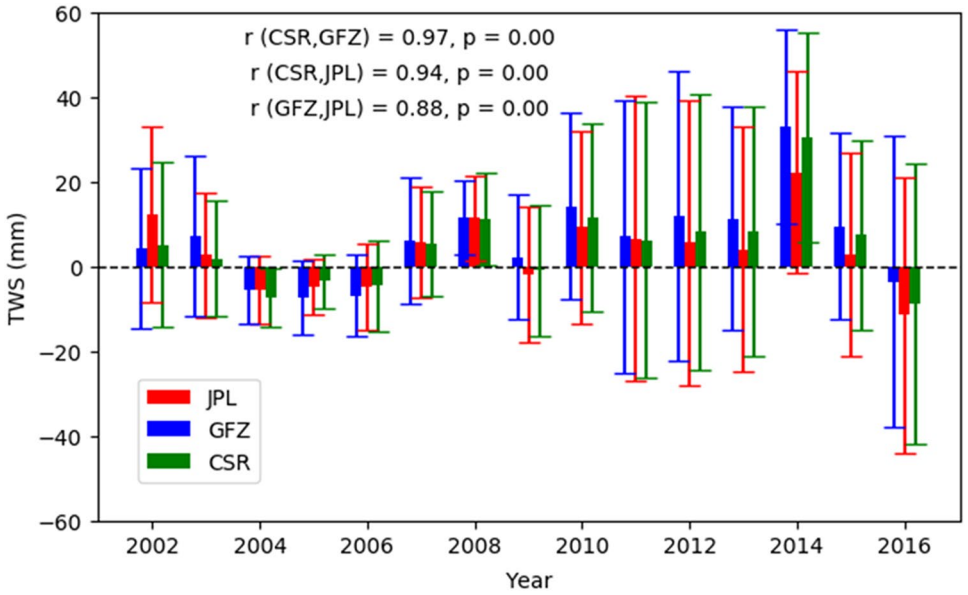

Fig. 2 Comparison of the three TWS data sources (CSR, GFZ, and JPL, units: mm) in NSSA during 2002–2016 with their respective standard deviations and the correlation coefficients

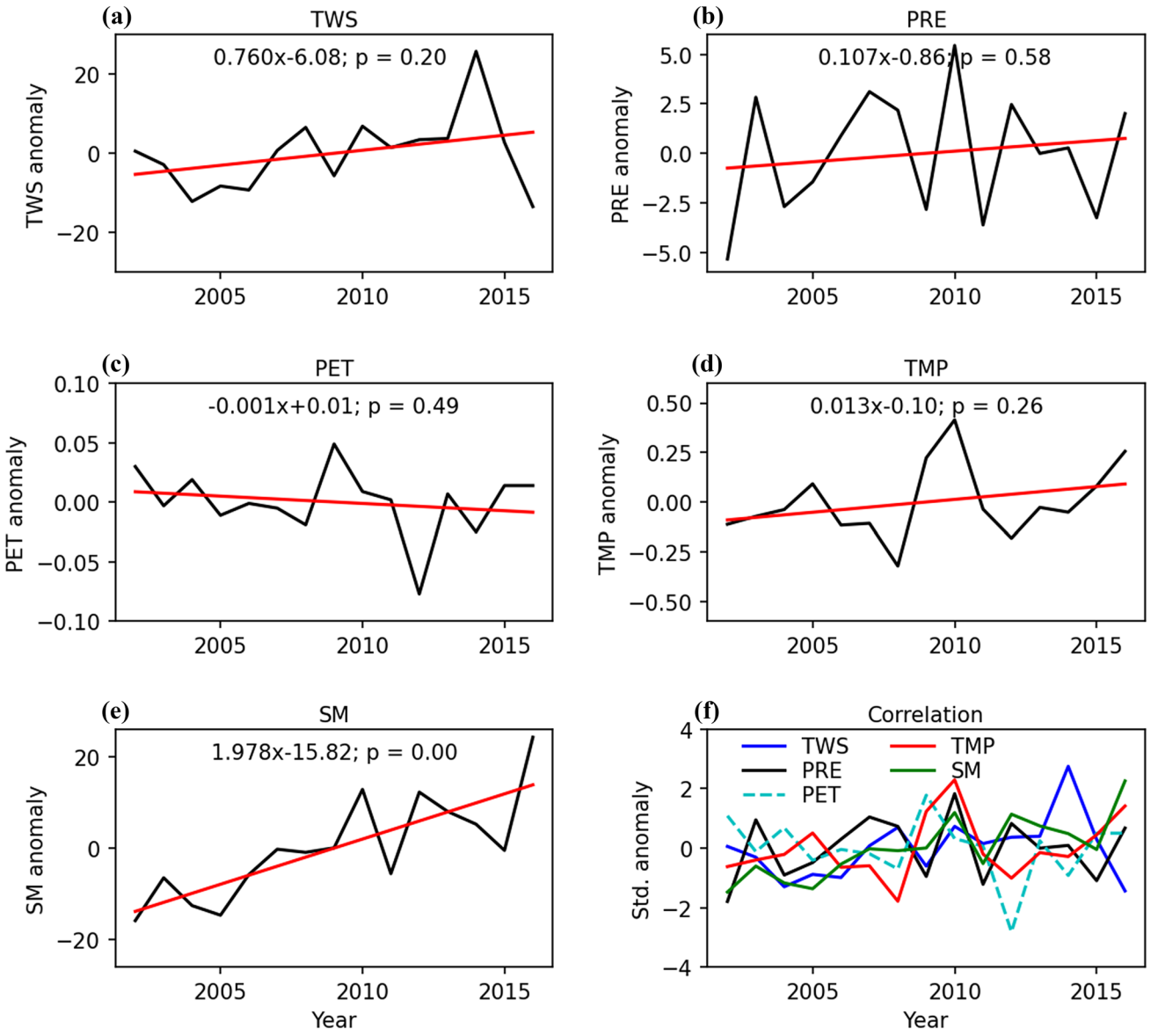

Fig. 3 Area average time series of annual **a** TWS (mm), **b** PRE (mm), **c** PET (mm day^{-1}), **d** TMP (°C), **e** SM (mm), and spatial correlations of **a** with **b** – **d** in **f**, respectively, for the period from 2002 to 2016. Std means standardized

who focused their study on the assessment of groundwater resources in the Iullemmeden Basin of West Africa and found an increase of 0.4 m per annual. The increasing trend in GRACE data was attributed to climate variations (Bridget et al. 2018). Also, the linear trend in TWS (Ndehedehe et al. 2017) over West Africa presented a positive change in total water resources, which is in agreement with the result of linear regression employed in our analysis.

A rising tendency of PRE was observed in the NSSA with a slope change rate of 0.107 mm year^{-1} with a $p = 0.58$ (Fig. 3b). Hence, the increasing trend in PRE was not significant at a 5% level. Previous studies (Marshall et al. 2012) reported that the precipitation projection showed a modest increase over the Sahel and East Africa that is similar to our finding. According to Maidment et al. (2015), observations exhibit rational upturns in annual Sahel precipitation (about 29–43 mm decade^{-1}), which partially agreed with the increase of the precipitation trend in the NSSA.

Concerning PET, a declining tendency was observed (Fig. 3c). The decreasing rate of − 0.001 mm day^{-1} year^{-1} was noticeable with $p = 0.49$, which was not significant at the 5% level. Xuening et al. (2012) discussed the possible causes of the decrease in the potential evapotranspiration in the Huaihe River (China). They found that precipitation and temperature increased while the potential evapotranspiration has decreased. They called the phenomenon

as "evaporation paradox" and attributed the causes to a decreasing tendency in wind speed. The decrease of wind speed in the NSSA could be the controlling factor inducing potential evapotranspiration's decline (Xuening et al. 2012). The slope change rate in TMP increased, with a value of 0.0130 °C year^{-1}. The increased slope change rate of TMP is not significant ($p = 0.26$). The increasing trend in TMP implied that the NSSA was realistically warmer (Fig. 3d). For illustration, a study found that areas in both North experienced significantly warmer temperatures in the most recent period 1995–2010 than in the period 1979–1994 (Collins 2011). Meanwhile, for the months from December to February, the significant warming concentrated in the northern part of Africa (Collins 2011). This result is in harmony with the findings of Aguillar et al., (2009) in Guinea Conakry and some central African countries. The SM exhibited an increasing tendency with an increased rate of 1.978 mm year^{-1}, which was significant ($p = 0.00$) (Fig. 3e). The increasing of soil moisture could be linked to weak evapotranspiration although temperature and precipitation raised weakly.

We used the standardized values of the climate variables and that of TWS for temporal correlation analyses (Fig. 3f) to circumvent the problem of units. An in-phase change between the TWS and PRE was observed with an $r = 0.17$, which was statistically insignificant ($p = 0.55$). The weak relationship between the precipitation and TWS had been attributed to a high effect of unaccounted evaporation and runoff (Awange et al. 2014). An out-of-phase relationship between the TWS and PET was obtained with a correlation coefficient of − 0.38, which was not statistically significant ($p = 0.16$). As well, a similar relationship (i.e., meant a negative correlation coefficient) was observed between the TWS and TMP. A weak correlation between TWS and TMP was acquired with an $r = -0.20$, which was statistically insignificant at a 5% level ($p = 0.48$). The assessment of trends of global water storage from GRACE showed a negative correlation between temperature and the inter-annual total water storage over Africa (Vincent Humphrey Humphrey et al. 2016), which is in agreement with the finding of the study. The association of TWS and SM demonstrated an in-phase oscillation with an $r = 0.19$ and $p = 0.49$. A study found that in normal years, the GRACE-TWS showed a strong connection and comparable characteristic time scale to surface SM, while in drier years, GRACE-TWS demonstrated stronger persistence, suggesting slower recovery time and elongated water supply restraint on vegetation growth (Geruo et al. 2017). The variations observed could be the signal of decadal; henceforth, cautions should be taken to drawing the conclusion.

3.2 Spatial Distribution of Trends in Total Water Storage Anomalies and Climate Variables

The trends based on the satellite observatory were not yet carried over the NSSA region. Figure 4 showed the spatial distribution of the linear trend in TWS and climatic variables (PRE, PET, TMP, and SM) during the period from 2002 to 2016. The Student's test at the common level (0.05) was used for the test of significance. It could be observed that the TWS over West Africa (approximately − 18° E to 15° E and 2°–20° N) experienced positive changes (Fig. 4a). The increasing trend observed in West Africa is similar to the findings of Humphrey et al. (2016) and Ndehedehe et al. (2016a; b) but used different techniques. Likewise, Long et al. (2017), found an increased trend mainly in Gambia and Niger basins. A large part of the countries, such as Niger, Sudan, and Ethiopia, also experienced an increasing trend in TWS. Meanwhile, the Central African countries, namely Cameroon, Central African Republic, South Sudan, the southern part of Chad, the Northern part of Niger, experienced negative trends in it. The average change per year of the entire NSSA was between 6.81 and − 5.03 mm year^{-1}. The negative change in TWS occupied 35.08%, whereas that of the positive occupied 56.59% of the total area. The proportion of areas that underwent significant positive changes was 44.76%, whereas the proportion of areas that underwent significant negative changes was 24.84%.

Areas of negative trends in PRE were nearly balanced with areas displaying increased trends in PRE over the entire NSSA (Fig. 4b). The southern part of Nigeria and the eastern part of Ethiopia showed significant decreasing trends in PRE at the 5% level. The coastal region (includes, Liberia, Ivory Coast, Ghana, Togo, Benin, Nigeria, and part western Cameroon) and South Sudan located between − 11° E to 12° E and 2° N to 12° N and 24° E to 34° E and 2° N to 10° N experienced negative trends in PRE. Meanwhile, a significant positive trend was found in PRE over the areas between 12° E to 24° E and 2° N to 17° N, 34° E to 46° E and 2° N to 14° N and the western Sahel (comprises eastern Mali, western Burkina-Faso, Sierra Leone, Guinea, Guinea-Bissau, and Gambia). The average change per year across the entire NSSA region was between 2.83 and − 7.45 mm year^{-1}. The negative change in PRE occupies 27.88% whereas the positive in it occupied 49.29% of the total area. The proportion of areas that underwent significant positive changes was 19.65%, whereas the proportion of areas that underwent significant negative changes was 9.49%.

Figure 4c displayed a heterogeneity of significant negative and positive trends in PET during the study period over the NSSA. Negative trends could be observed in areas situated nearly between − 5° E to 5° E and 12° N to 15° N (western Niger, central-eastern of Mali, northern Burkina-Faso) over part of West Africa. Also, negative

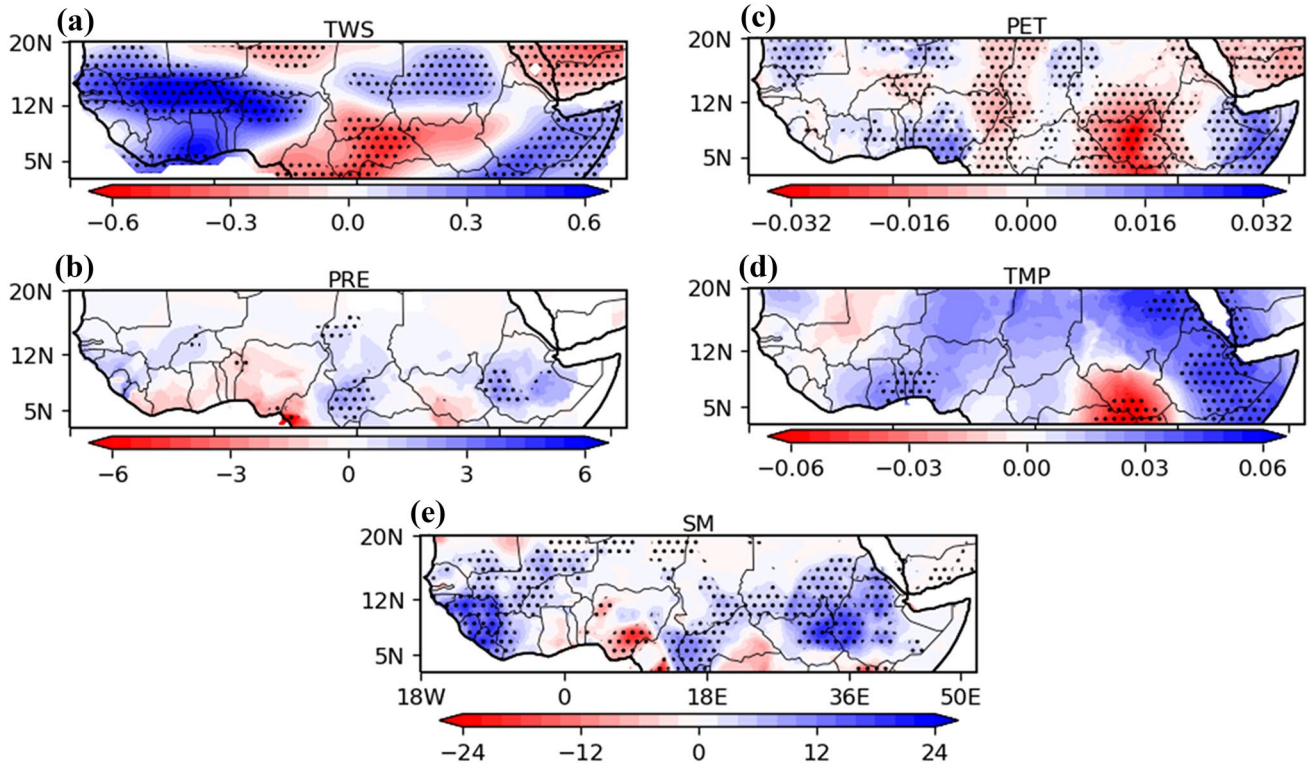

Fig. 4 Spatial distribution of linear trends in **a** TWS (mm year^{-1}), **b** PRE (mm year^{-1}), **c** PET (mm day^{-1} year^{-1}), **d** TMP (°C year^{-1}), and **e** SM (mm year^{-1}) during 2002–2016. Dots indicate significance at the 5% level

trends in PET were obtained in East and Central Africa, areas located between 10° E to 17° E and 2° N to 20° N (includes northeastern Nigeria, Cameroon, Western Chad, and northeastern Niger) and 24° E to 40° E and 2° N to 20° N (includes, Sudan, South Sudan, and western Ethiopia). Remaining parts of NSSA exhibit positive trends in PET encompassing smaller areas compared with areas of negative trends in PET. The result suggested that over the NSSA, there were dominant significant negative trends in PET. The average change over the entire NSSA was between 0.021 and − 0.40 mm day^{-1} year^{-1}. Adverse changes in PET occupied 49.21%, whereas positive variations of it occupied 36.37% of the total area. The proportion of areas that underwent significant positive changes was 15.84%, whereas the proportion of areas that underwent significant negative changes was 26.22% of the total area.

Figure 4d showed significant localized trends in TMP. Regions of significant positive trends in TMP include Ethiopia, Horn of Africa, southwestern Nigeria, South Benin, Togo, and Eastern Ghana while South Sudan with its southern countries' borders showed significant negative trends. The average change over the whole NSSA was between 0.05° and − 0.06°C year^{-1}. The negative change in TMP occupied 16.25%, whereas the positive change in it occupied 69.68% of the total area. The proportion of areas that underwent significant positive changes was 38.07%, whereas the proportion of areas that underwent significant negative changes was 6.03%.

Figure 4e exhibited mixt trends in SM during the study period. Significant positive trends in SM featured most of the areas. Strong decreasing trends observed over Nigeria could be explained partly by the rise in temperature, which drove to high evaporation, hence loss of water storage. It was sustained by the decrease of precipitation regardless of the significance. The average change of the all-inclusive NSSA was between 19.96 and − 27.79 mm year^{-1}. The negative change in SM occupied 30.85%, whereas that of the positive change in it occupied 55.40% of the total area. The proportion of areas that underwent significant positive changes was 45.07%, whereas the proportion of areas that underwent significant negative changes was 20.24%.

3.3 Leading Modes and their Temporal Variability of Total Water Storage Anomaly

The EOF analysis based on the singular value decomposition method was used in the present study to extract the leading modes of the total water storage variability after removing the annual cycle from the original data. The EOFs patterns are represented as regression maps of TWS anomalies onto

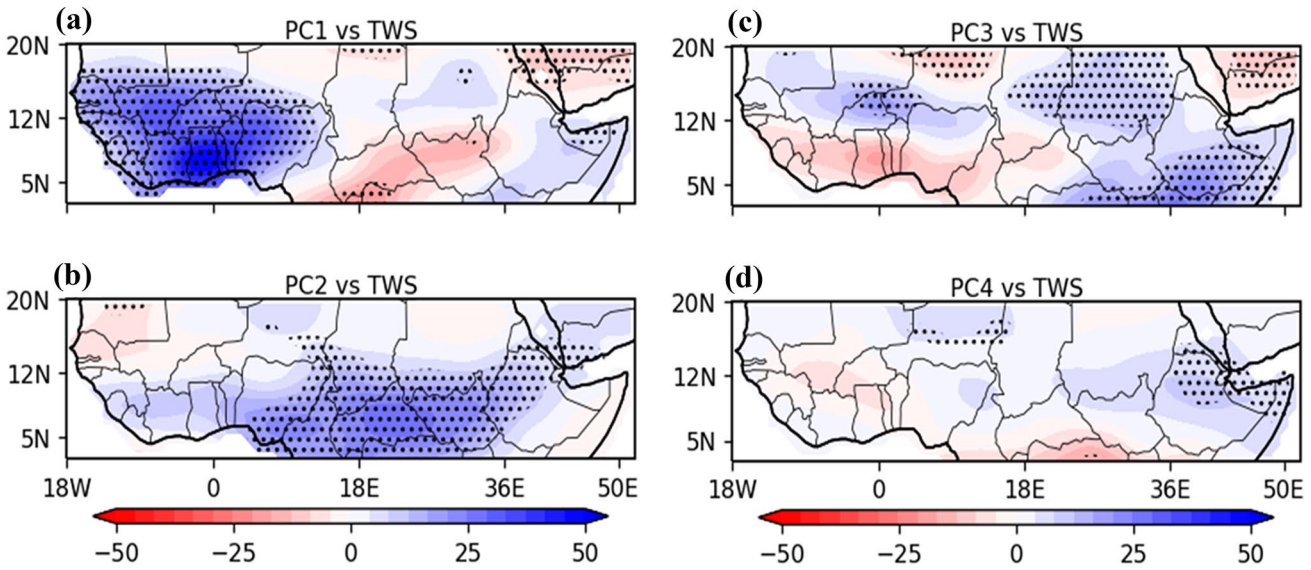

Fig. 5 Regression maps of the TWS anomaly (mm) onto **a** PC1, **b** PC2, **c** PC3 and **d** PC4 from 2002 to 2016. Dots indicate significance at the 5% level

PCs (Fig. 5). The EOF1 explained 46% of the total TWS variance that described the anomalous TWS pattern (Fig. 5a). It characterized the highest variability in TWS over the NSSA. The EOF2 explained 25.86%, which featured the anomalous TWS pattern (Fig. 5b). The EOF3 (Fig. 5c) and the EOF4 (Fig. 5d) explained 16.73% and 4.6% of the total variance in TWS anomalies, respectively, and characterized the lowest variability in TWS anomaly in the NSSA. Figure 5a depicted positive relationships of TWS and PC1 indicating a positive change in TWS. These significant relationships were found in West Africa (including, for example, Nigeria, Benin, Togo, Burkina-Faso, Senegal, and Conakry Guinea). Average maximum and minimum slope change rates of 50.23 and − 22.22 mm year^{-1} were observed in TWS, respectively. A negative association of TWS and PC1 was observed over Cameroon, Central African Republic, and South Sudan. The percentage of negative (positive) variability of TWS was 33.17% (58.49%) of the total area, respectively. Among negative (positive) changes, 8.02% (28.81%) were significant at the 5% level, respectively. As depicted by the PC1, the year 2012 corresponded to one of the broadest spread West African floods (IRIN 2013).

The variability of PC2-TWS was displayed in Fig. 5b. Significant positive variations could be seen over areas including Nigeria, southern Chad, Cameroon, Central African Republic, South Sudan, southernmost Sudan, and northern-western Ethiopia. Parts of southern Mauritania experienced significant negative variations in TWS. The percentage of negative (positive) variability of TWS was 20.56% (71.11%) of the total area, respectively. Meanwhile, the variations ranged between − 6.68 and 28.49 mm. Among negative (positive) changes, 0.87% (29.92%) were significant at the 5% level, respectively. Figure 5c showed the regressed PC3-TWS. Positive significant variations in TWS were apparent over northern Burkina-Faso, southern Niger, central-eastern Mali, central-eastern Chad, Sudan, southern Ethiopia, and Eritrea. It was noted that the northern part of Niger experienced significant variations in TWS. The percentage of negative (positive) variability of TWS was 35.24% (56.43%) of the total area, respectively. Meanwhile, the variations ranged between − 18.59 and 27.89 mm. Among negative (positive) changes, 6.43% (24.37%) were significant at the 5% level, respectively.

From Fig. 5a, d few locations experienced significant variations in TWS, which includes the northern part of Niger, the northern part of Ethiopia, and Eritrea. These points of negative variations in TWS were statistically significant. The percentage of negative (positive) changes in TWS is 27.38% (64.29%) of the total area, respectively. Meanwhile, the variations oscillated between − 17.38 and 9.34 mm. Among negative (positive) changes, 0.63% (7.86%) were significant, respectively. The PCs of the first four leading EOF modes were shown in Fig. 6. The four EOF modes retained, accounts for 93.19% of the variance in TWS. The previous study used the technique of principal component analysis to extract time variations modes TWS in West Africa and found a total explained variance of 72.2% accounting for the first four leading modes (Ndehedehe et al. 2016a; b), which percentage is less than ours. The technique or the time spanning of the study could explain the difference observed. Irrespective of the accounting percentage, the increasing tendency of the first mode was apparent.

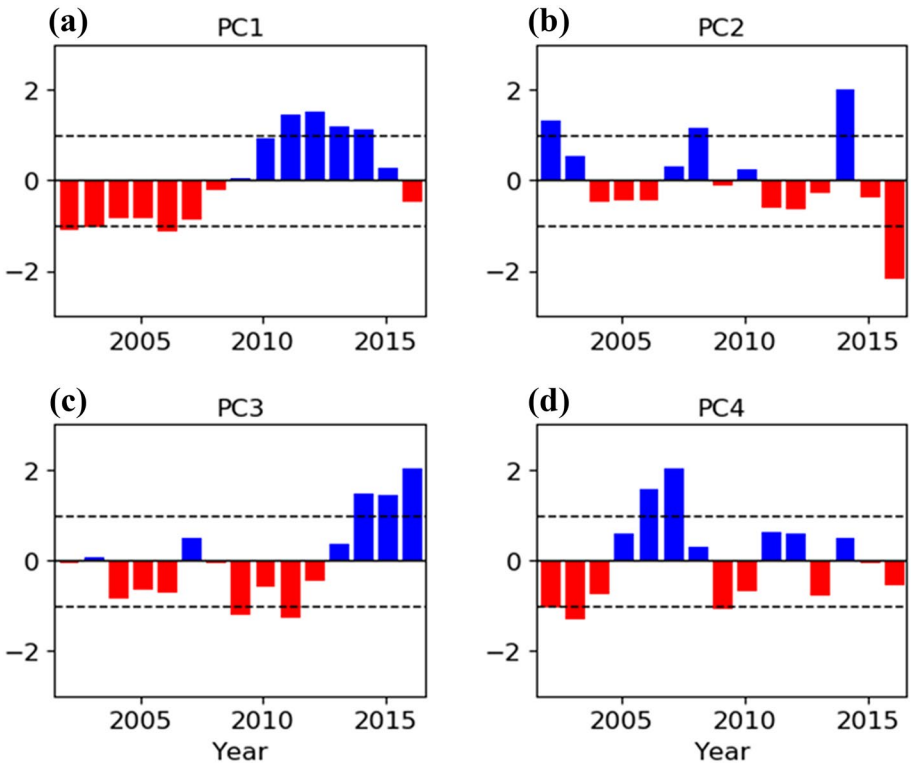

Fig. 6 PCs of the first four modes of TWSA in NSSA; **a** PC1, **b** PC2, **c** PC3, and **d** PC4. Y-axis stands for the standardized amplitude of PCs. The horizontal dashed lines indicate standardized PCs greater than absolute values of 1

Table 1 Years of water deficit and surplus in NSSA indicated by the PCs of its TWS during 2002–2016

	PC1	PC2	PC3	PC4
W +	2011, 2012, 2013, 2014	2002, 2008, 2014	2014, 2015, 2016	2006, 2007
W −	2002, 2003, 2006	2016	2009, 2011	2002, 2003, 2009

The W + denotes water surplus and W − denotes water deficit

Standardized TWS-PCs time series with absolute values greater than 1 are selected as surplus and deficit years and presented in Table 1, which is similar in meaning of standardized precipitation anomaly or standardized precipitation index (Ogwang et al. 2015). The adoption of this technique follows Thomas et al. (2014), who used the monthly TWS anomalies to characterize the water deficit of regions, such as Amazon and Zambezi River basins, and the southeastern United States and Texas regions. Moreover, Zhao et al. (2016) have exposed that the drought severity index of GRACE performed well at temporal and spatial scales in capturing the meteorological drought indices during 2002 − 2014 in the continental Unites States. Therefore, the following Table 1 is drawn to present the period of deficit and surplus of water storage over NSSA during the period 2002–2016 based on the standardized PCs magnitudes from the EOF analysis. While 2009 was detected in this study as a deficit year, it was reported as a water surplus in Ouagadougou (Engel et al. 2017), the year 2012 was confirmed by our findings describing the water surplus in Dakar (Engel et al. 2017). Furthermore, the year 2012 of water surplus was also confirmed by the past severe flood in West Africa (IRIN 2013) as shown spatially.

3.4 Spatial Distribution of Change in Total Water Storage in Responses to Climate Variables Changes

The regression of TWS onto time series of other variables is useful for water resources prediction and monitoring. Figure 7 depicted the variations of TWS in relation to change in time series of PRE, PET, TMP, and SM during 2002–2016. TWS was regressed over the hydro-climatic variables anomalies (standardized anomalies). Non-significant changes at the 5% level were found between changes in TWS and PRE for the study period (Fig. 7a). However, a positive association of TWS with PRE was observed over most of the areas, while a small area experienced a negative correlation. Indeed, the area of the negative relationship between TWS and PRE covered Sierra Leone, part of Liberia, southern and

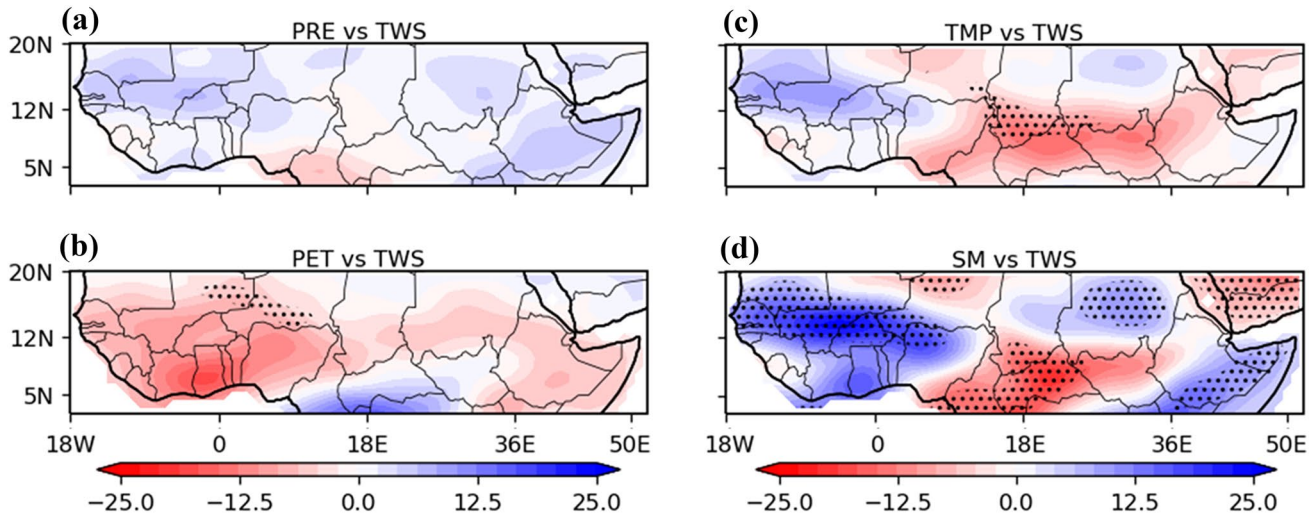

Fig. 7 Regression maps of TWS (mm year^{-1}) onto standardized time series of **a** PRE, **b** PET, **c** TMP, and **d** SM for the period 2002 − 2016. Dots indicate the significance at the 5% level

southeastern Nigeria, Cameroon, Central African Republic, southern to southwestern Chad, including Lake Chad. It could also be seen that small parts of southern Benin, southern Togo, and a circular area within South Sudan showed a negative association of TWS with PRE. It meant an increase of PRE was linked to a decreasing in TWS over small parts of the NSSA while over most parts of the area (NSSA); an increase in PRE was interconnected with an increase in TWS. The maximum and minimum linear trends of TWS were 6.66 mm year^{-1} and − 6.41 mm year^{-1}, respectively. Adverse associations of PRE with TWS occupied 17.62%, whereas positive relations of them occupied 74.05%. The negative relationship between PRE and TWS could be explained by the fact that the storage water is enough that additional water could not increase the storage volume, but instead flowed as runoff. Furthermore, human water withdrawal could explain the situation as well. It meant that the water used by human activities increase more than the quantity of water received from precipitation, which is the primary source of water in the region.

Figure 7b presented the relationship between PET and TWS for the period of study. Few whereabouts showed a significant negative association of TWS with PET at the 5% level. A small area of insignificant positive of the association was evident, which encompassed Cameroon, Central African Republic, South Sudan, and northern Congo. As an illustration, the finding over northern Congo was in agreement with that of Crowley et al. (2006) who found a decreasing tendency of total water storage with an increase in evaporation and runoff. Meanwhile, the rest of the area showed a negative relationship between changes in PET and TWS. That meant that an increase in PET was associated with a decrease in total water storage due to the loss of water. The minimum slope rate of TWS in response to variations in PET was found to be − 17.53 mm year^{-1}, and the maximum change rate of TWS concerning variations in PET was 16.52 mm year^{-1}. The area percentage occupied by negative relationships between PET and TWS was 72.78% against 18.89% for a positive relationship. Among the percentage of the negative relationships, 2.62% was statistically confident but 0.00% for significant positive changes.

The distribution of TMP changes associated with TWS changes was shown in Fig. 7c. The negative correlation of TMP and TWS was apparent over most parts of the NSSA. However, a few locations underwent a significant change at the 5% level. The positive correlation between TWS and TMP covered the areas, such as from central to northern Sudan, northern Chad, southern Niger, western Nigeria, northern Benin, northern Togo, northern Ghana, eastern Ivory Coast, northern Guinea, Senegal, southern Mali, and southern Mauritania. The increase of TWS was associated with an increase in TMP. That could be real under the conditions that an increase in TMP led to an increase in precipitation because of the direct link between the precipitation and the water storage. NASA (2019) reported that an increase in the average global temperature possibly led to variations in precipitation and atmospheric moisture, comprising moves towards more extreme precipitation during storms. (Humphrey et al., 2016) did a similar study by analyzing the correlation between GRACE data and temperature at the global scale, and the result depicted a large area with non-significant correlation coefficients (Humphrey et al., 2016). The maximum and minimum correlations of TWS to fluctuations of TMP were 9.75 mm year^{-1} and − 14.33 mm year^{-1}, respectively, over the whole area. Adverse associations of TMP and TWS occupied 58.17%,

whereas positive associations of them occupied 33.49%. Among the percentage of the negative relationships, 4.29% was statistically confident against 0.0% statistically significant at the 5% level.

Heterogeneous but significant responses of variations in TWS to changes in SM were observed during 2002–2016 in the NSSA (Fig. 7d). A maximum change rate of 23.96 mm year^{-1} of TWS was achieved while a minimum change rate of − 20.21 mm year^{-1} of it was acquired over the region. The significant anti-correlation at the 5% level between SM and TWS was obtained over the areas that include Cameroon, Central African Republic, South Sudan, and northern Niger. Besides, insignificant anti-correlations of TWS with SM were gotten in northwestern Ethiopia and northern Mali. Negative responses of TWS to SM implied that when SM increases, the TWS decreases, signifying that the SM moisture was not a determinant factor for total water storage in most of the central African countries. This could be explained by the saturated soil cannot retain more water. A significant in-phase relationship of TWS and SM was obtained in southern Ethiopia, Sudan, southwestern Niger, Burkina-Faso, Senegal, Mali, Southern Mauritania, and northwestern Nigeria. Besides, non-significant responses of TWS to SM were apparent in Benin, Togo, Ghana, Ivory Coast, Liberia, Guinea, and Guinea-Bissau. It meant that the soil moisture could be used to estimate the water resource over most of the West African countries because an increase in SM led to an increase in TWS. Hence, SM was a determinant factor of total water storage over West Africa. Negative associations of SM with TWS occupied 38.17%, whereas positive associations of them occupied 53.49%. Among the percentage of the negative relationships, 13.97% was statistically confident against 19.84% statistically significant at the 5% level in Africa (IRIN, 2013) as shown spatially.

3.5 Spatial Patterns of Trends in Water Budget and its Components from GLDAS Datasets

The spatial trend analysis is carried out on the GLDAS model outputs to its performance for monitoring water resources over the NSSA. Figure 8 displayed the trends of the water budget elements and water budget estimated for the period from 2002 to 2016 in the NSSA. Variations of water resources components were carried out using the linear regression method. In general, changes in runoff (Ro) were uninformed over the area (Fig. 8a). Dominant positive change of Ro was palpable (70.28% of the total area). Few localities exhibited a significant change in Ro during the period of study. Areas, such as Nigeria, from central to southern Benin, western Cameroon, and Togo, experienced negative changes regarding Ro (29.72% of the total area). Meanwhile, negative changes in Ro were not significant at the 5% level. Spatial variations of trends in Ro during 2002–2016 range from 0.14 to − 0.02 mm day^{-1} year^{-1}. Significant positive trends in Ro occupied 17.06% against 3.37% for significant negative trends. A study of runoff trend at global scale showed an increase of runoff over the eastern equatorial of Africa (Milly et al. 2005), which is consistent with our result from the trend of runoff at the spatial scale.

A large area of the region showed significant positive trends of ET (Fig. 8b), it meant that 90.40% of the total area experienced a positive change in ET while a small area (9.60%) showed a negative change in ET during the period of the study. The maximum and minimum slope change rates in ET over the region were 0.18 mm day^{-1} year^{-1} and

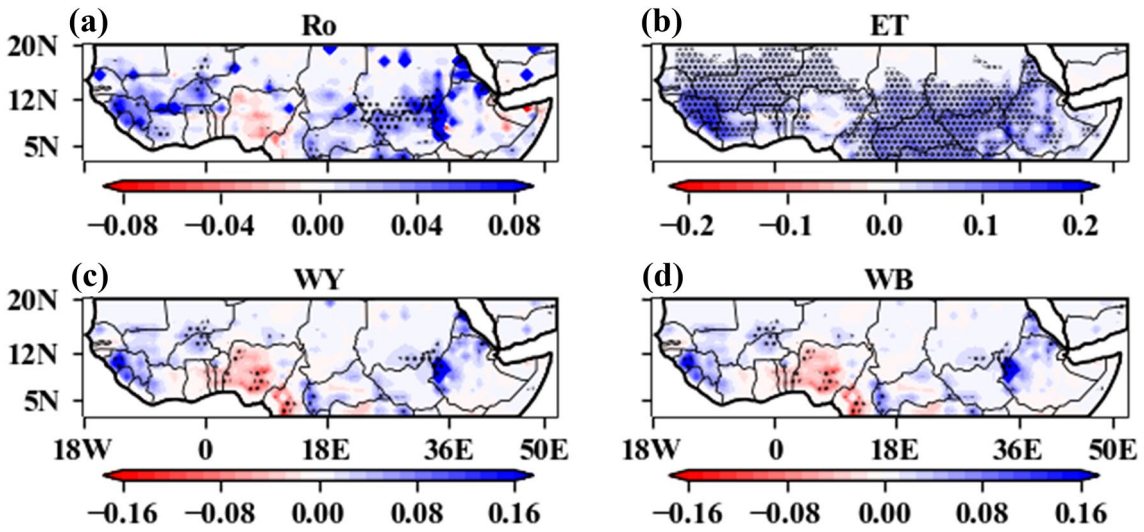

Fig. 8 Spatial distribution of linear trends in **a** Ro (mm day^{-1}), **b** ET (mm day^{-1}), **c** WY (mm day^{-1}), and **d** WB (mm day^{-1}) during 2002–2016 over NSSA. Dots indicate significance at the 5% level

−0.05 mm day^{-1} year^{-1}, respectively. Significant positive trends in ET occupied 63.94% against 1.33% for significant negative trends. In Fig. 8c, d, the slope changes in WY and WB were presented. The patterns of the spatial distribution of trends in WY and WB were almost identical. However, the magnitude of changes in WB was less than that of changes in WY. The maximum change rate of WY was 0.35 mm day^{-1} year^{-1}, and the minimum slope change rate of it was −0.17 mm day $^{-1}$ year^{-1}. Besides, the maximum slope change rate of WB was 0.28 mm day^{-1} year^{-1}, and the minimum slope change rate of it was −0.17 mm day^{-1} year^{-1}. The trends in WY and WB were heterogeneous. The proportions of negative changes in WY and WB were 35.65% and 36.06%, respectively, whereas the proportions of positive changes in WY and WB were 64.35% and 63.9, respectively. Moreover, the percentage of the area experiencing a positive (negative) significant change in WY was 10.62% (3.88%) correspondingly. Concerning the WB, areas that experienced positive (negative) changes were 10.21% (3.88%), respectively. The runoff has contributed to the reduction of the water budget by 0.41%. A high ET contributes to a reduction of water resources in the NSSA region.

3.6 Relationship Between Area-Averaged Runoff, Total Evapotranspiration, and the Estimated Water Budget

Figure 9 showed the trends in Ro, ET, and WB during 2002–2016 in the NSSA. A positive trend was observed in Ro, ET, and WB. The trend in Ro was 0.001 mm day^{-1} year^{-1} and significant at the 5% level ($p = 0.00$). It was consistent with Huntington (2006), who found that the runoff increases at the regional and global scales. The increase of Ro would be due to the increase in precipitation with low storage of water. The increase in Ro was somewhat attributed to fluctuations in mean temperature, but also, the land-use change played the strongest role in increasing Ro in tropical regions (Piao et al. 2007). Similarly, a significantly positive trend in ET was achieved with a change rate of 0.035 mm day^{-1} year^{-1} with $p = 0.00$. The increase of ET could be attributed to the increase of RF owing to the increase in temperature. The increased trend in ET is in accordance with the results from the study of Huntington (2006). A non-significant increase tendency was obtained in the WB. The Slope change rate of WB was 0.004 mm day^{-1} year^{-1} with $p = 0.37$. The increase in precipitation could explain the increase of WB because it has resulted from the difference between precipitation and total evapotranspiration and runoff.

Based on Pearson's correlation, a significant positive connection of WB with Ro was revealed ($r = 0.65$ and $p = 0.01$). The correlation between the Ro and ET was positive significant at the 5% level ($r = 0.81$, $p = 0.00$). An insignificant and positive correlation coefficient between WB and ET was obtained ($r = 0.31$, $p = 0.26$). A significant increase tendency was observed in RF during the period of study. A slope change rate of 0.04 mm day^{-1} year^{-1} in RF was acquired with $p = 0.00$. From these results, an increase in WB could be associated with an increase in RF. The positive deficit of the water budget would be in the origin of floods events in the region, which is consistent with IWMI (2010) that reported that changes in precipitation would increase variability in groundwater recharge and river flow, thus affecting all water sources. The negative deficit would be explained by the role of evaporation that tends to lower the water level in a wetland over time, and evapotranspiration acted to dry out the soil before the next storm (Erickson et al. 2010).

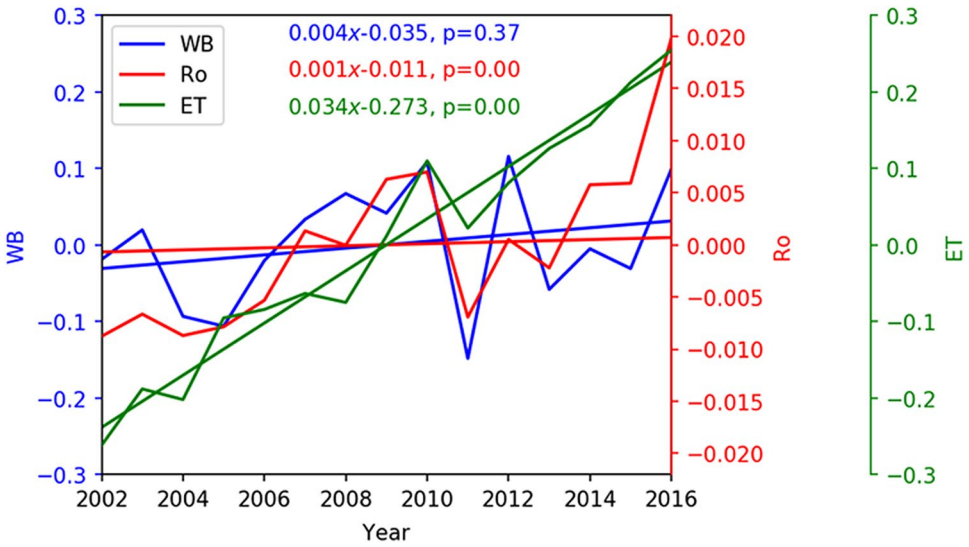

Fig. 9 Time series (curves) of changes in the Ro (mm day^{-1}), ET (mm day^{-1}), and WB (mm day^{-1}) and their linear regression (straight lines) for the period 2002 − 2016

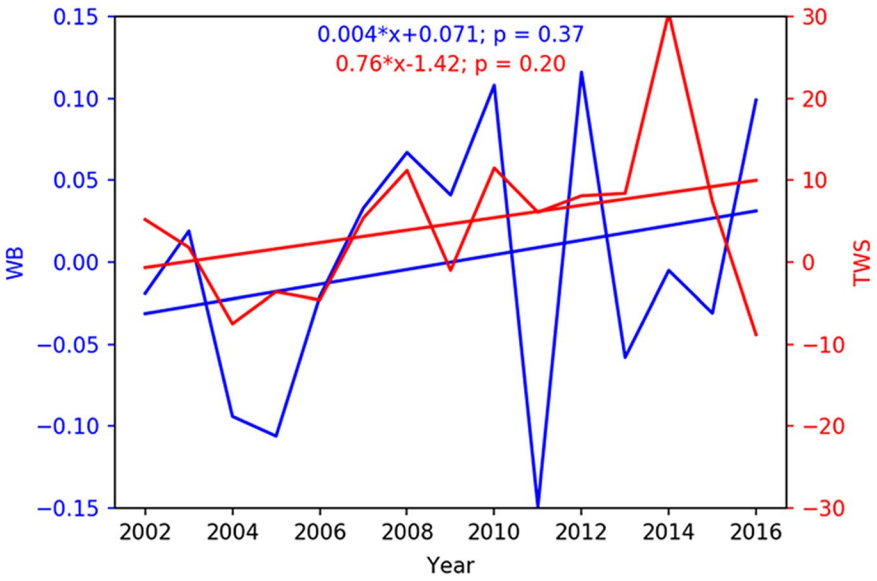

Fig. 10 Time series (curves) and linear regression (straight lines) of WB (mm day^{-1}) and TWS (mm) changes

3.7 Relationship Between Area-Averaged Total Water Storage and Estimated Water Budget

Despite the discrepancies of area average, time series is useful and easy to predict the future. Figure 10 presented variations of the time series of WB and the TWS and the relationship between them. Both TWS and WB showed increase tendencies. The tendency in TWS was not significant at the 5% level, as well, that of WB was not significant at this level. Slope change rates of WB and TWS were 0.004 mm day^{-1} year^{-1} (0.004 × 30 days = 0.12 mm year^{-1}) and 0.76 mm year^{-1} for WB and TWS, respectively. The lowest amount (−0.149 mm day^{-1} year^{-1}) of WB was found in 2011, whereas the highest amount (0.116 mm day^{-1} year^{-1}) was detected in 2012. The lowest amount (−88 mm) of TWS was obtained in 2016, whereas its highest amount (304 mm) was obtained in 2014. The correlation of TWS anomaly with WB anomaly exhibits a non-significant relationship ($r = 0.14$, $p = 0.61$). It meant that there was low evidence proving that an increase of WB was significantly associated with an increase of TWS.

As per Khawaja (2012), Sub-Saharan Africa experienced a severe drought in 2011 that caused damages to agricultural activities during 2011–2012, which seemed to coincide well with the negative water budget obtained in the present study. Furthermore, the low variability (PC3) of total water storage depicted 2011 as a water-deficit year. A study by Kuss et al. (2012) had made a comparison between a simulated groundwater change and GRACE in California and found that there was a significant difference between the changes in the two parameters at the river and the land levels. It was consistent with the weak relationship found between WB and TWS. The difference observed was attributed to the limit of GRACE's spatial resolution (Kuss et al. 2012). However, in the current study, for the fact that similar resolutions were used, the difference could be due to the technique of processing the data or the weak coverage of stations used to measure the precipitation in the area.

3.8 Relationships Between the Total Water Storage and Water Budget and NDVI Anomalies

The correlation of NDVI with the TWS and water budget (WB) was calculated and shown in Fig. 11. It should be mentioned that the spatial resolution of the NDVI variable was interpolated to 1° × 1° resolution to match that of TWS and WB. In Fig. 11a, both positive and negative correlations were obtained. Of these correlations, 46.59% were positive, whereas 31.43% were negative. At the 10% level, significant

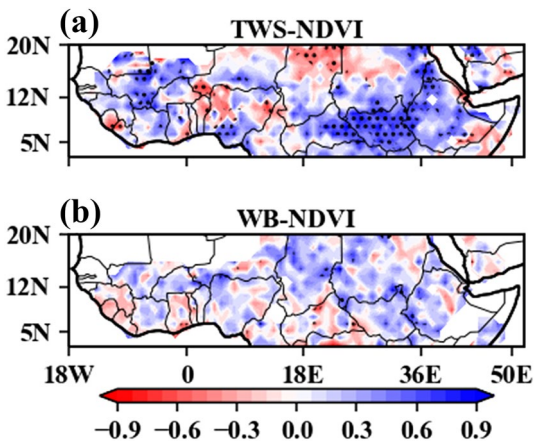

Fig. 11 Spatial distribution of correlation coefficients of NDVI with TWS and WB during 2002–2015. Dots indicate the significance at the 10% level. White parts are the areas with no data

positive (negative) correlations occupied 13.41% (7.38%), respectively. It meant most plants in NSSA were interdependent on the TWS. The result is in harmony with the findings of Xie et al. (2019). Figure 11b displayed the relationship between the WB and the vegetation change. The results indicated dominant positive association coefficients between NDVI and WB during the period from 2002 to 2015. Positive correlations occupied 37.86%, whereas negative correlations occupied 28.49%. Of these proportions, 5.08% (3.49%) of positive (negative) correlations were significant. Similarly, it meant that the development of many plants over the area (NSSA) inevitably relied on the WB.

This is in line with previous findings, which argued that the GRACE-TWS was a better indicator for greenness (Yang et al. 2014; Andrew et al. 2017). However, a study showed that soil moisture offers the paramount illustration of the actual quantity of water accessible for plants (Yang et al. 2014). It was found that changes in water availability strongly affect vegetation growth, and vegetation can also modify land water storage by changing the land surface water balance (Xie et al. 2019). That showed that the interactions of NDVI with water resources (i.e., WB and TWS) are complex and have a non-unique direction. The GRACE-TWS was importantly associated with vegetation cover compared to the WB estimated from the GLDAS model outputs over the period 2002–2016 in the NSSA region.

4 Conclusion

Changes in water resources in relation to hydro-climatic and NDVI variables were investigated during 2002–2016 over the NSSA region. Moreover, based on the simple water balance equation, we estimated the water yield (WY) and water budget (WB). After examining the relationship of WB with runoff and the total evapotranspiration (ET), we compared WB with TWS and evaluated their interdependence to show the degree of agreement between them. Empirical orthogonal functions (EOF), linear regression, and correlation were applied in the assessment. The conclusions are as following:

- The analysis of changes in hydro-climatic variables showed increasing trends in precipitation, temperature, soil moisture, TWS, WB, runoff, and ET, whereas a decreasing trend was observed in potential evapotranspiration.
- Based on the EOF, the GRACE-TWS was able to detect extreme events specifically floods over West Africa in the NSSA region; hence, it can be used for disaster management.
- Positive associations were found between the TWS and hydro-climatic variables and between WB and TWS, Ro and ET. It means when the hydro-climatic variable increases, the water resource increases.
- The relationship between the estimated water budget from the GLDAS model and the TWS is positive but not significant at the 5% level.
- The examination of the relations of NDVI with TWS and WB showed a significant association, meaning that the water resources, such as TWS and WB, are determinant factors for vegetation growth.

These findings are useful for water resource and environmental management especially in the era of climate change.

Acknowledgements We acknowledge the CAS-TWAS program under which we have acquired more knowledges in the field of earth sciences. We thank Professor Zhugguo Ma and the associate professor Francois Cossi Guedje for their advices during our Ph.D. program and after the Ph.D, respectively. We are grateful for the data providers for free without which the present work won't be possible. Our special thanks to the anonymous reviewers and editors for their helpful comments for improvement of the manuscript.

Author contributions The design, methodology and first draft of the present manuscript are worked out by FKO. It is revised by VNO, EN and CIM.

Declarations

Conflict of interest The authors declare no conflict of interest.

References

Andrew RL, Guan H, Batelaan O (2017) Large-scale vegetation responses to terrestrial moisture storage changes. Hydrol Earth Syst Sci 21(9):4469–4478. https://doi.org/10.5194/hess-21-4469-2017

Awange JL, Forootan E, Kuhn M, Kusche J, Heck B (2014) Water storage changes and climate variability within the Nile Basin between 2002 and 2011. Adv Water Resour 73:1–15. https://doi.org/10.1016/j.advwatres.2014.06.010

Bolten J et al (2012) Looking to the future: forming a comprehensive GRACE FO applications strategy. Presented at the 2012 GRACE Science Team Meeting, Potsdam, Germany

Bridget RS, Zizhan Z, Himanshu S, Alexander YS, Hannes MS, Ludovicus PHVB, David NW, Yoshihide W, Di L,Robert CR, Laurent L, Petra D, Marc FPB (2018) Global models underestimate large decadal declining and rising water storage trends relative to GRACE satellite data. PNAS 115(6):E1080–E1089. https://doi.org/10.1073/pnas.1704665115.

Carter RC, Parker A (2009) Climate change, population trends in Africa. Hydrol Sci J 54(4):676–689. https://doi.org/10.1623/hysj.54.4.676

Carvalho R, Longuevergne T, Gurdak L, Jason J, Leblanc M, Favreau G, Aureli A (2018) Assessment of the impacts of climate variability on total water storage across Africa: implications for groundwater resources management. Hydrogeol J. https://doi.org/10.1007/s10040-018-1864-5

Collins JM (2011) Temperature variability over Africa. J Clim 24(14):3649–3666. https://doi.org/10.1175/2011JCLI3753.1

Cosgrove B, Walker JP, Gottschalck J, Houser PR, Mitchell K, Jambor U, Rodell M (2004) The global land data assimilation system. Bull Am Meteorol Soc 85(3):381–394. https://doi.org/10.1175/bams-85-3-381

Crowley JW, Mitrovica JX, Bailey RC, Tamisiea ME, Davis JL (2006) Land water storage within the Congo Basin inferred from GRACE satellite gravity data. Geophys Res Lett 33(19):2–5. https://doi.org/10.1029/2006GL027070

Deser C, Blackmon ML (1995) On the relationship between tropical and North Pacific sea surface temperature variations. J Clim 8(6):1677–1680. https://doi.org/10.1175/1520-0442(1995)008%3c1677:OTRBTA%3e2.0.CO;2

Dool HVD Huang J, Fan Y (2003) Performance and Analysis of the constructed analogue method applied to US soil moisture applied over 1981–2001. J Geophys Res 108:1–16

Du J, Shu J, Yin J, Yuan X, Jiaerheng A, Xiong S, He P, Liu W (2015) Analysis on spatio-temporal trends and drivers in vegetation growth during recent decades in Xinjiang, China. Int J Appl Earth Obs Geoinf 38:216–228. https://doi.org/10.1016/j.jag.2015.01.006

Engel T, Fink AH, Knippertz P, Pante G, Bliefernicht J (2017) Extreme Precipitation in the West African Cities ofDakar and Ouagadougou: atmospheric Dynamics and Implications for Flood Risk Assessments. J Hydrometeorol,18(11):2937–2957. https://doi.org/10.1175/JHM-D-16-0218.1

Erickson AJ, Gulliver JS, Hozalski RM, Mohseni O, Nieber JL, Wilson BN, Weiss PT (2010) Stormwater Treatment:assessment and Maintenance. In University of Minnesota, St. Anthony Falls Laboratory

Famiglietti JS, Rodell M (2013) Water in the balance. Sci 340(6138):1300–1301. https://doi.org/10.1126/science.1236460

Feng XM, Sun G, Fu BJ, Su CH, Liu Y, Lamparski H (2012) Regional effects of vegetation restoration on water yield across the Loess Plateau. China Hydrol Earth Syst Sci 16(8):2617–2628. https://doi.org/10.5194/hess-16-2617-2012

Geruo A, Velicogna I, Kimball JS, Du J, Kim Y, Colliander A, Njoku E (2017) Satellite-observed changes invegetation sensitivities to surface soil moisture and total water storage variations since the 2011 Texas drought. Environ Res Lett, 12(5). https://doi.org/10.1088/1748-9326/aa6965

Gizaw MS, Gan TY (2017) Impact of climate change and El Niño episodes on droughts in sub-Saharan Africa. Clim Dyn 49(1–2):665–682. https://doi.org/10.1007/s00382-016-3366-2

Guenang GM, Vondou DA, Kamga FM (2016) Total Water Storage Change in Cameroon: calculation, Variability and Link with Onset and Retreat Dates of the Rainy Season. Hydrol. 1–19. https://doi.org/10.3390/hydrology3040036

Guillaume F, Yahaya N, Marc L, Goni AG, Ibrahim B (2011) Groundwater resources increase in the Iullemmeden Basin, West Africa. In Climate Change Effects on Groundwater Resources: a Global Synthesis of Findings and Recommendations pp 113–128

Grippa M, Kergoat L, Frappart F, Araud Q, Boone A, De Rosnay P, Lemoine JM, Gascoin S, Balsamo G, Ottlé C,Decharme B, Saux-Picart S, Ramillien G (2011) Land water storage variability over West Africa estimated by Gravity Recovery and Climate Experiment (GRACE) and land surface models. Water Resour Res, 47(5):1–18. https://doi.org/10.1029/2009WR008856

Hannachi A (2004) A primer for EOF analysis of climate data. Reading: University of Reading, 1–33. http://www.o3d.org/eas-6490/lectures/EOFs/eofprimer.pdf. Accessed 20 June 2021

Harris I, Jones PD, Osborn TJ, Lister DH (2014) Updated high-resolution grids of monthly climatic observations -the CRU TS3.10 Dataset. Int J Climatol, 34(3), 623–642. https://doi.org/10.1002/joc.3711

Humphrey V, Gudmundsson L, Seneviratne SI (2016) Assessing Global Water Storage Variability from GRACE:trends, Seasonal Cycle, Subseasonal Anomalies and Extremes. Surv Geophys, 37(2), 357–395. https://doi.org/10.1007/s10712-016-9367-1

Huntington TG (2006) Evidence for intensification of the global water cycle: Review and synthesis. J Hydrol, 319(1–4), 83–95. https://doi.org/10.1016/j.jhydrol.2005.07.003

IRIN. (2013) Preparing for floods in West Africa. In The New Humanitarian: Environment and Disasters. https://www.thenewhumanitarian.org/news/2013/06/14/preparing-floods-west-africa

Jiang L, Jiapaer G, Bao A, Guo H, Ndayisaba F (2017) Vegetation dynamics and responses to climate change and human activities in Central Asia. Sci Total Environ 599–600:967–980. https://doi.org/10.1016/j.scitotenv.2017.05.012

Jonah K, Wen W, Shahid S, Ali MA, Bilal M, Habtemicheal BA, Iyakaremye V, Qiu Z, Almazroui M, Wang Y, Joseph SN, Tiwari P (2021) Spatiotemporal variability of rainfall trends and influencing factors in Rwanda. J Atmos Solar-Terrestrial Phys 219:105631. https://doi.org/10.1016/j.jastp.2021.105631

Khawaja M (2012) Drought in Sub-Saharan Africa puts millions of lives at risk. Arabian Gazette. https://arabiangazette.com/sub-saharan-drought-risk/

Kuss A, Brandt W T, Randall J, Floyd B, Bourai A, Newcomer M, Schmidt C, Skiles JW (2012) Comparison ofchanges in groundwater storage using GRACE data and a hyrdological model in California's central Valley. ASPRS2012 Annu Conf, PP 1–12 .

Landerer FW, Swenson SC (2012) Accuracy of scaled GRACE terrestrial water storage estimates. WaterResources Research, 48(4):1–11.https://doi.org/10.1029/2011WR011453

Long D, Yang YT, Guan HD, Scanlon BR, Simmons CT, Jiang L, Xu X (2017) GRACE satellite observed hydrological controls on interannual and seasonal variability in surface greenness over mainland Australia. JGeophys Res Biogeosciences, 119: 2245–2260

Lv M, Ma Z, Li M, Zheng Z (2019) Quantitative analysis of terrestrial water storage changes under the Grain for Green program in the Yellow River basin. Geophys Res Atmos 124:1336–1351. https://doi.org/10.1029/2018JD029113

Maidment RI, Allan RP, Black E (2015) Recent Observed and Simulated Changes in Precipitation over Africa.Geophys Res Lett, 42, 8155-8164. https://doi.org/10.1002/2015GL065765.

Marshall M, Funk C, Michaelsen J (2012) Examining evapotranspiration trends in Africa. Clim Dyn 38(9–10):1849–1865. https://doi.org/10.1007/s00382-012-1299-y

Milly PCD, Dunne KA, Vecchia AV (2005) Global pattern of trends in streamflow and water availability in a changing climate. Nature 438(7066):347–350. https://doi.org/10.1038/nature04312

NASA (2019) Precipitation measurement missions. Retrieved from https://pmm.nasa.gov/science/climate-change. Accessed 20 June 2021

Ndehedehe CE, Awange J, Agutu NO, Kuhn M, Heck B (2016a) Advances in water resources understanding changes in terrestrial water storage over West Africa between 2002 and 2014. Adv Water Resour 88:211–230. https://doi.org/10.1016/j.advwatres.2015.12.009

Ndehedehe CE, Agutu NO, Okwuashi O, Ferreira VG (2016b) Spatiotemporal variability of droughts and terrestrial water storage over Lake Chad Basin using independent component analysis. J Hydrol 540:106–128. https://doi.org/10.1016/j.jhydrol.2016.05.068

Ndehedehe CE, Awange JL, Kuhn M, Agutu NO, Fukuda Y (2017) Climate teleconnections influence on West Africa's terrestrial water storage. Hydrol Process 31(18):3206–3224. https://doi.org/10.1002/hyp.11237

Ogou KF, Ma Z, Yang Q, Kpaikpai B (2017) Comparison of trends and frequencies of drought in central North China and sub-Saharan Africa from 1901 to 2010. Atmos Ocean Sci Lett 10(6):418–426. https://doi.org/10.1080/16742834.2017.1392825

Ogwang BA, Chen H, Tan G, Ongoma V, Ntwali D (2015) Diagnosis of East African climate and the circulation mechanisms

associated with extreme wet and dry events: a study based on RegCM4. Arab J Geosci 8(12):10255–10265. https://doi.org/10.1007/s12517-015-1949-6

Petheram C, Walker G, Grayson R, Thierfelder T, Zhang L (2002) Towards a framework for predicting impacts of land-use on recharge: 1, a review of recharge studies in Australia. Aust J Soil Res 40(3):397–417

Piao S, Friedlingstein P, Ciais P, de Noblet-Ducoudré N, Labat D, Zaehle S (2007) Changes in climate and land use have a larger direct impact than rising CO2 on global river runoff trends. Proc Natl Acad Sci USA 104(39):15242–15247. https://doi.org/10.1073/pnas.0707213104

Pinzon JE, Tucker CJ (2014) A non-stationary 1981–2012 AVHRR NDVI3g time series. Remote Sens 6(8):6929–6960. https://doi.org/10.3390/rs6086929

Reager JT, Famiglietti JS (2009) Global terrestrial water storage capacity and flood potential using GRACE. Geophys Res Lett 36(23):2–7. https://doi.org/10.1029/2009GL040826

Thomas AC, Reager JT, Famiglietti JS, Rodell M (2014) A GRACE-based water storage deficit approach for hydrological drought characterization. Geophys Res Lett 41(5):1537–1545. https://doi.org/10.1002/2014GL059323

Tom TH, Alison HP, Weatherhead EK (2012) Testing a rapid climate change adaptation assessment for water and sanitation providers in informal settlements in three cities in sub-Saharan Africa. Environ Urbaization 24(2):619–637. https://doi.org/10.1177/0956247812453540

Xie X, He B, Guo L, Miao C, Zhang Y (2019) Detecting hotspots of interactions between vegetation greenness and terrestrial water storage using satellite observations. Remote Sens Environ 231:111259. https://doi.org/10.1016/j.rse.2019.111259

Xuening MA, Mingjun Z, Yaju LI, Shengjie W, Qian MA, Wenli LIU (2012) Decreasing potentialevapotranspiration in the Huanghe River Watershed in climate warming during 1960–2010. J Geogr Sci 22(6):977–988. https://doi.org/10.1007/s11442-012-0977-3

Yang YT, Long D, Guan HD, Scanlon BR, Simmons CT, Jiang L, Xu X (2014) GRACE satellite observed hydrological controls on interannual and seasonal variability in surface greenness over mainland Australia. J Geophys Res Biogeosciences 119:2245–2260

Yang Z, Zhang Q, Hao X (2016) Evapotranspiration trend and its relationship with precipitation over the loess plateau during the last three decades. Adv Meteorol. https://doi.org/10.1155/2016/6809749

Zhang X, Wu S, Yan X, Chen Z (2017) A global classification of vegetation based on NDVI, rainfall and temperature. Int J Climatol 37(5):2318–2324. https://doi.org/10.1002/joc.4847

Zhao C, Li X, Zhou X, Zhao K, Yang Q (2016) Holocene vegetation succession and response to climate changeon the south bank of the heilongjiang-amur river, mohe county, northeast China. Adv Meteorol. https://doi.org/10.1155/2016/2450697